DEVELOPMENT OF PRECIPITATION AND CLOUD PRODUCTS FROM ATOVS/AVHRR DATA AT SMHI

A. Thoss[1], R. Bennartz[2] and A. Dybbroe[1]

[1]Swedish Meteorological and Hydrological Institute
Norrköping, Sweden
[2]Institut for Space Sciences, Free University of Berlin
Berlin, Germany

1. INTRODUCTION

At SMHI methods and software to retrieve cloud and precipitation information from data of the new generation of operational meteorological satellites is being developed. The work is carried out mainly in the framework of the "Eumetsat Satellite Application Facility (SAF) to support Nowcasting and Very Short Range Forecasting". The Nowcasting SAF (SAFNWC) is scheduled to end in February 2002, with the delivery of two integrated software packages for the Meteosat Second Generation (MSG) and European Polar System (EPS) satellites.

The main delivery of SMHI will be new methods and software for the extraction of four high latitude (applicable north of 50°N) cloud and precipitation products based on AVHRR and AMSU data. The four products will be:

- AVHRR Cloud Mask
- AVHRR Cloud Type
- Cloud Top Temperature/Height
- Precipitating Clouds from both AVHRR and AMSU

In the following we provide an overview of the Cloud Mask product and discuss the development of the Precipitating Clouds product in more detail.

2. AVHRR CLOUD MASK

The central aim of the AVHRR Cloud Mask (CMa) is to delineate absolutely cloud free pixels in a satellite scene with a high confidence. The CMa scheme is a thresholding scheme using a number of

spectral and textural image features derived from all available AVHRR channels. In order to adapt to the actual environmental conditions the scheme employs dynamic thresholds depending on the surface characteristics (land, sea and coast), the sun-satellite viewing geometry, the total integrated water vapour content and the surface temperature. The thresholds are primarily derived from off-line radiative transfer simulations using the RTTOV model (Eyre, 1991 and Brunel et al. 1995) for the IR channels and the 6S (Tanré et al., 1990) for the visible and near infrared channels. The visible and near-infrared calculations include the model of sunglint on the ocean surface as described by Cox and Munk (1954).

A training database with classifications done by experienced meteorologists has been used for further fine tuning of some of the thresholds as for example the $T_{ch4} - T_{surface}$ thresholds. Even though adjustments like this are necessary, the principle angular dependence of the thresholds is well modelled by both RTTOV and 6S. Threshold images are pre-calculated for the actual scene using NWP model output for determining the integrated water vapour content and surface temperature.

Depending on scene and illumination conditions different sequences of tests are performed. There are different test sequences for sea, coast, land and high terrain. Also low level inversion cases (forecasted $T_{950} - T_{surface} > 0°C$) and possible sunglint cases are treated separately. For the selection of appropriate tests it is necessary to take into account illumination conditions. Considering the above mentioned scene dependencies we currently divide processing into:

- 7 Night time algorithms
- 8 Twilight algorithms (solar zenith angle 80°-95°)
- 6 day time algorithms

Besides the five main output categories non-processed, cloud free, cloud filled, cloud contaminated, snow/ice contaminated, and unclassified, the Cloud Mask product also includes a 16 bit threshold test flag and a 16 bit quality flag. The quality flag includes information on the degree of confidence in the thresholding, so that if a pixel has a value close to a threshold in one of the image features the pixel will be assigned a low confidence.

More details on the AVHRR Cloud Mask can be found in Dybbroe et al (1999). Currently the performance of the cloud mask is monitored on a real time basis. Results over sea are very satisfying, whereas over land some further tuning is needed, especially concerning twilight and high terrain.

3. THE PRECIPITATING CLOUDS PRODUCT

Particularly over land surfaces, the retrieval of instantaneous precipitation rates from passive microwave observations might be associated with large uncertainties. Using VIS/IR imagery, the retrieval of instantaneous rain rates is even more uncertain and the spatial extent of the precipitation usually gets overestimated. To make better use of the actual information content of the remotely sensed data, an approach was chosen to provide likelihood estimates of precipitation in different intensity intervals. The precipitation likelihood for different predictors will be inferred from co-located radar data, which has been adjusted to rain gauges.

The Precipitating Clouds product will give the likelihood of precipitation in four intensity classes:

- No precipitation (rain rate < 0.1mm/h)
- Risk of precipitation/ light precipitation (0.1 – 0.5mm/h)
- Light to medium precipitation (0.5 – 5mm/h)
- Strong precipitation (> 5mm/h)

A match-up database has been build up containing AVHRR, AMSU and co-located radar data for the period April – September 1999 in the Baltic Area. An example case from the database is given in Figure 1.

3.1 The AVHRR product

The AVHRR part of the Precipitating Clouds (PC) product will consist of two steps. First possibly precipitating clouds will be selected from the results of the cloud type classification. An overall precipitation likelihood of the different cloud types is inferred for each cloud type. Cloud free areas will be assigned a 100% probability of no precipitation. For pixels exhibiting any chance of precipitation, further predictors will be investigated.

Assuming that cloud microphysical properties like the effective droplet radius are likely to be correlated with precipitation (Rosenfeld and Gutman, 1994), a retrieval algorithm for the effective cloud droplet radius has been developed. Radiative transfer simulations for the 0.6μm, 1.6μm and the solar scattered part of the 3.7μm channel have been performed for a wide range of cloud micro-physical properties and viewing geometries using an adding and doubling model. Mie theory was applied to both water and ice droplets. For the inversion of the radiative transfer simulations a neural backpropagation network was chosen. Results of the simulations show that it is not possible to retrieve both the cloud phase and the effective radius with good accuracy if only the 0.6μm and 3.7μm channel are present. When applying networks trained on the wrong cloud phase to the simulation dataset,

biases in the retrieved radii of up to several μm occur. If the cloud phase is uncertain, neural nets trained without phase discrimination performed best.

First applications of the neural net to satellite data gave a realistic distribution of effective radii, but the overall magnitude seems too large. For some scenes the effective radius was well correlated with radar echoes, whereas for other scenes this was not the case. Further, more detailed investigations are currently under way.

As further predictors to enhance the AVHRR PC product the difference of cloud top temperature and forecasted ground temperature and the 0.6μm reflectance will be considered.

3.3 AMSU Products

In the microwave region precipitation can be detected either by its emission signal for frequencies below about 60GHz (over water surfaces only) or for frequencies above 60GHz by the scattering signature of frozen precipitation. Using a radiative transfer model considering only absorption, but including polarisation and the change of polarisation state with zenith angle, we performed radiative transfer simulations for a set of about 1000 globally well distributed radiosonde profiles. Based on the simulations for AMSU-A channels at 23GHz and 31GHZ, regression algorithms for water vapour path and liquid water path over sea were developed.

The retrieval of the water vapour path has the form

$$w = a + b \cdot \log(290 - t23) + c \cdot \log(290 - t31) \qquad (1)$$

where w is the water vapour path, t23 and t31 are the AMSU-A brightness temperatures at 23GHz and 31GHz respectively and a, b and c are coefficients depending on the observation geometry. The theoretical accuracy of the algorithm is 1.5kg/m^2 . Applying the algorithm to AMSU-A data and verifying the results with co-located radiosondes gave an rms error of 2.5kg/m^2 and a bias of +0.5kg/m^2.

The retrieval of cloud liquid water path (LWP) has the form

$$lwp = a + b \cdot t31 + c \cdot t23 + d \cdot \log(290 - t23) \qquad (2)$$

where lwp is the liquid water path, and a, b, c and d are coefficients depending on the observation geometry. The theoretical retrieval accuracy varies with zenith angle and lies between 0.018kg/m^2 and 0.025kg/m^2. Since LWP retrievals are difficult to verify, only a consistency check was applied to real data. The LWP was derived for fields of view which were identified as cloud free from AVHRR pixels. This means that the average retrieved LWP should be close to 0.0kg/m^2 and the distribution

should only have small tails on either side of zero. These requirements were well met with an average retrieved LWP of 0.005kg/m^2 and an rms of 0.015kg/m^2.

The radiative transfer modelling described above would give a basis for the development of emission based precipitation retrieval over sea for AMSU-A. It would however be difficult for us to verify results with the BALRAD radar network since only few AMSU-A pixels over the Baltic Sea can be regarded as not contaminated by land surfaces.

For AMSU-B only scattering based algorithms can be considered. The higher spatial resolution of AMSU-B is also more adequate to detect precipitation, since it is more likely that a high percentage of the field of view is filled with precipitation as compared to AMSU-A. Since a large percentage of our available ground truth radar lies over land or coastal areas, we can also take advantage of the fact that scattering based algorithms can be adapted for use over land. Two scattering indices were investigated: SI89 refers to AMSU-B 89GHZ –AMSU-A 23GHz, SI150 refers to AMSU-B 150GHz – AMSU-A 23GHz.The percentage of correctly identified precipitation events increases with rain rate for both SI89 and SI150 (see Figure 2 for precipitation retrievals over sea, Figure 3 for precipitation over land). For rain rates of less than 0.5mm/h the AMSU retrievals are quite uncertain and only about 50% to 60% of the light rain events according to radar data are identified as raining by AMSU (Tables 1-3). The reason for this lies mainly in the insensitivity of the AMSU data to light precipitation, but also some artefacts in the radar data like ground clutter or anomalous propagation might cause erroneous "precipitation".

In general SI150 exhibits a higher skill to identify precipitation (Figures 1 and 2, Tables 1 and 2). This is most likely due to the higher optical thickness of the frozen precipitation at 150GHz.

Precipitation estimates over land perform slightly worse than over sea, but when using the 150GHz scattering index the estimates are still very useful. The percentage of correctly identified precipitation with rain rates of more than 0.5mm/h only decreases from 91% over sea to 88% over land. More severe is the misclassification of dry events as raining, which increases from 6% over sea to 18% over land (Tables 1 and 2).

As further development the output of the algorithms will be translated to precipitation probabilities in certain intensity intervals. As soon as we have gathered enough cases to contain ice and snow cover we will have to develop quality control algorithms for winter conditions to account for scattering of snow and ice covered surfaces. A further step will be to transfer the locally tuned algorithm to other geographical areas. An adjustment to the Spanish radar network is already planned.

References

Brunel, P., L. Lavanant and G. Rochard, 1995: Infrared transmittance database for fast radiative transfer model. Proc. 8th International TOVS Study conference, 5-11 April,1995, Queenstown, New Zeeland.

Cox, C. and W. Munk, 1954:Measurements of the roughness of the sea surface from the suns's glitter, J.Opt. Soc. Am. 44, 838-850.

Eyre, J., 1991:A fast radiative transfer model for satellite sounding systems, ECMWF Tech.Memorandum No. 176.

Dybbroe, A., K.-G. Karlsson, A. Thoss, 1999: The AVHRR Cloud Mask scheme of the SAFNWC. Proc. 1999 EUMETSAT Data Users Conference, September 1999, Copenhagen. Publ. EUMETSAT, in press.

Rosenfeld,D. and G. Gutman, 1994:Retrieving microphysical properties near the tops of potential rain clouds by multispectral analysis of AVHRR data. Atmospheric Research 34, 259 – 283.

Tanré, D., C. Deroo and P. Duhaut, 1990: Description of a computer code to simulate the satellite signal in the solar spectrum: the 5S code. Int. J. Rem. Sens., 11, 659-668.

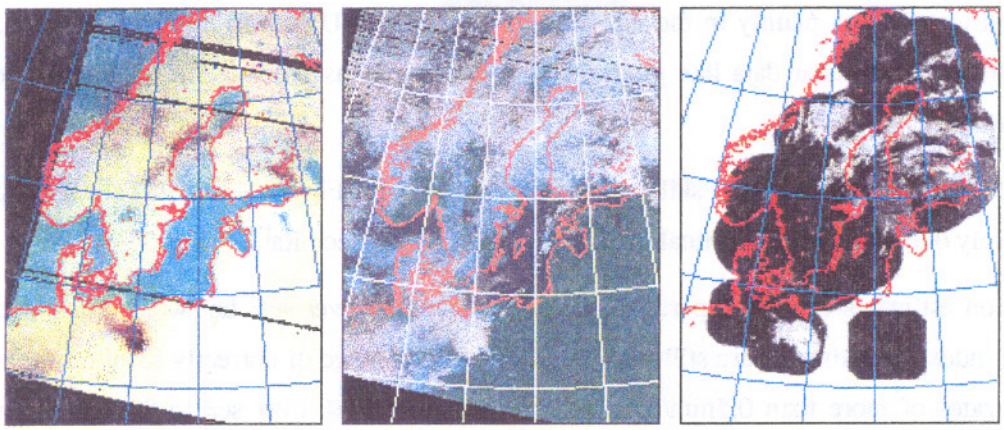

AMSU-RGB	AVHRR-RGB	BALTRAD
89,150,183±7 GHz	CH 4,2,1	radar composite

Fig.1 Example content of the AMSU/AVHRR/Radar database: NOAA-15 overpath 6 July 1999, 6:44 UT

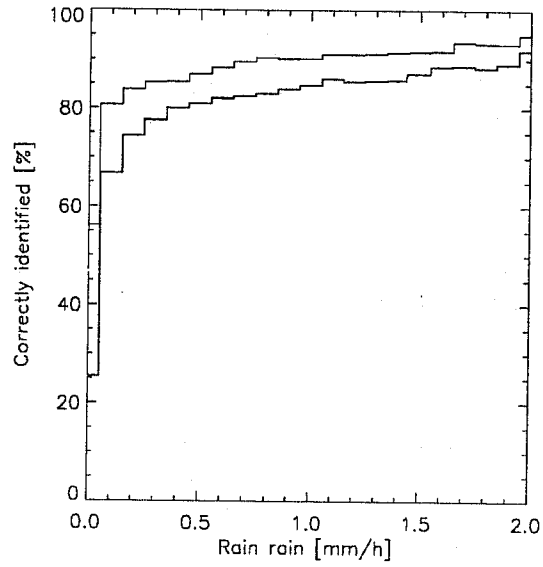

Fig.2 Percentage of correctly identified precipitation events over sea depending on radar rain rate. Upper line for 150GHz scattering index, lower for 89GHz scattering index.

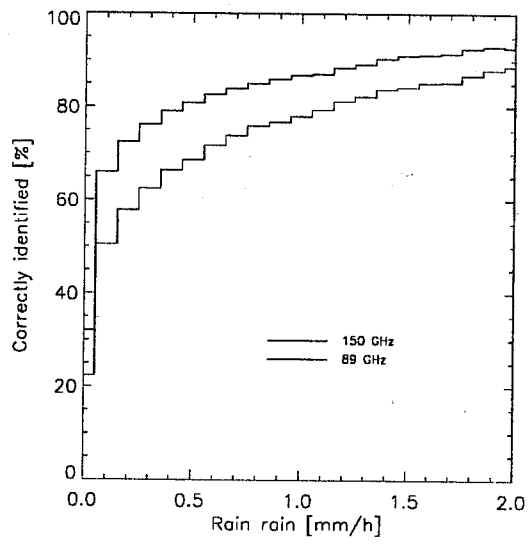

Fig.3 Percentage of correctly identified precipitation events over land depending on radar rain rate. Upper line for 150GHz scattering index, lower for 89GHz scattering index.

SEA Radar ⇒ ⇓150GHz retrieval	**No rain** Cases: 5281	**Rain > 0.5mm/h** Cases: 1625	**Rain < 0.5mm/h** Cases: 488
No Rain	93.7	9.2	44.9
Rain	6.3	90.8	55.1

Tab. 1 Contingency tables for rain rate retrieval over sea using 150GHz.

SEA Radar ⇒ ⇓89GHz retrieval	**No rain** Cases: 5281	**Rain > 0.5mm/h** Cases: 1625	**Rain < 0.5mm/h** Cases: 488
No Rain	77.2	18.1	38.4
Rain	22.8	81.9	61.6

Tab. 2 Contingency tables for rain rate retrieval over sea using 89GHz .

LAND Radar ⇒ ⇓150GHz retrieval	**No rain** Cases: 38234	**Rain > 0.5mm/h** Cases: 8832	**Rain < 0.5mm/h** Cases: 2696
No Rain	82.4	12.1	48.0
Rain	17.6	87.9	52.0

Tab. 3 Contingency table for rain rate retrieval over land using 150GHz .